Tests of the Radiation Hardness of VLSI Integrated Circuits and Silicon Strip Detectors for the SSC Under Neutron, Proton, and Gamma Irradiation

H.J. Ziock, C. Milner, W.F. Sommer,
Los Alamos National Laboratory, Los Alamos, NM 87545

N. Cartiglia, J. DeWitt, D. Dorfan, B. Hubbard, J. Leslie, K.F. O'Shaughnessy, D. Pitzl, W.A. Rowe, H.F.-W. Sadrozinski, A. Seiden, E. Spencer, P.Tennenbaum
Santa Cruz Institute for Particle Physics, University of California, Santa Cruz, CA 95064

J. Ellison, S. Jerger, C. Lietzke and S.J. Wimpenny
University of California, Riverside, CA 92521

P. Ferguson
University of Missouri-Rolla, Rolla, MO 65401

P. Giubellino
INFN, Torino, Italy

Abstract

As part of a program to develop a silicon strip central tracking detector system for the Superconducting Super Collider (SSC) we are studying the effects of radiation damage in silicon detectors and their associated front-end readout electronics. We report on the results of neutron and proton irradiations at the Los Alamos National Laboratory (LANL) and γ-ray irradiations at U.C. Santa Cruz (UCSC). Individual components on single-sided AC-coupled silicon strip detectors and on test structures were tested. Circuits fabricated in a radiation hard CMOS process and individual transistors fabricated using dielectric isolation bipolar technology were also studied. Results indicate that a silicon strip tracking detector system should have a lifetime of at least one decade at the SSC.

1. INTRODUCTION

At the SSC design luminosity of $10^{33}/cm^2sec$, the very high fluence of particles ($\approx 10^{14}/cm^2$ charged particles, an equal number of γ-rays, and a few times $10^{13}/cm^2$ neutrons) expected to be seen in one decade by a silicon strip tracking system at an inner radius of 15 cm will require systems of very high radiation resistance. The electronics associated with the detector elements will be mounted either directly on those elements or be an integral part thereof, and thus will be subjected to the same radiation dose. In a program to develop a silicon microstrip central tracking detector system for the SSC, we are studying the effects of radiation damage in silicon detectors and their associated front-end readout electronics. We report here on results of neutron and proton irradiations at LANL and γ-ray irradiation at UCSC. The devices tested included single-sided AC-coupled silicon strip detectors, and test structures. We determined the radiation tolerance of the components found on the detector surface and damage effects in the bulk silicon including donor removal. The readout electronics presently designed use two technologies: an amplifier/comparator stage built in bipolar technology for low noise, low power consumption, and high speed; and a data buffering stage built in radiation hard CMOS VLSI technology for low power consumption. The effect of radiation on the gain of bipolar transistors, and simple functioning CMOS circuits was investigated.

2. IRRADIATION FACILITIES

The irradiations by protons and neutrons used the beams produced at the Clinton P. Anderson Meson Physics Facility (LAMPF) at LANL. The kinetic energy of the primary LAMPF proton beam is 800 MeV with beam currents of 1mA. The proton exposure used a small extracted fraction of the 800 MeV beam. The neutron exposure was performed in the Los Alamos Spallation Radiation Effects Facility (LASREF) [1], which is associated with the beam stop for the primary beam. The energy spectrum of the neutrons at LASREF is similar to that expected to be seen by a central detector at the SSC. At both locations the neutron spectrum peaks at an energy of approximately 1 MeV or less, but has long tails going to higher and lower energies. LASREF reproduces much more of those tails than either reactor or radioactive neutron sources. Fluences equal to or greater than those expected at the SSC can be easily obtained.

To determine the proton and neutron fluences we used foil activation measurements. For the proton fluence the reactions $^{27}Al + p \rightarrow {}^{22}Na + X$ and $^{27}Al + p \rightarrow {}^{7}Be + X$ and the known cross section for those reactions at 800 MeV were used. The neutron fluences were determined in a similar fashion but using numerous different foils and reactions, as we also had to unfold the energy spectrum of the neutrons. Our analysis of the neutron fluence is not yet complete. A preliminary neutron

fluence Φ_n was obtained from the observed increase in leakage current in a photodiode:

$$I = I_o + \Phi_n \alpha_n A d \quad (1)$$

where I_o is the initial leakage current (about 0.3 nA), A·d is the diode volume, and a neutron damage constant of $\alpha_n = 6.6 \times 10^{-17}$A/cm is used [2]. That damage constant was determined for ^{235}U fission neutrons using identical photodiodes at 20°C. The ambient temperature in the beam stop ranged from 30 to 38°C, as measured by a thermocouple and a thermistor. Diode leakage currents were reduced to their value at 20°C assuming a temperature dependence of

$$I \sim T^2 \exp(-E/2kT) \quad (2)$$

with E = 1.2eV [3]. Both diode contacts were grounded during irradiation. The neutron flux was uniform over the area of the devices. The same technique was also used to determine proton fluences at intermediate times during the proton irradiations. In that case a value $\alpha_p = 4.8 \times 10^{-17}$A/cm was used.

The photon irradiation studies were performed in the ^{60}Co source at UCSC, which provides a dose rate of 25kRad/h in silicon. The source consists of 8 parallel rods each 20cm long arranged in circle of 9 cm radius, thus providing uniform irradiation over the entire sample area. During irradiation, the devices were placed into individual "filter boxes" consisting of 2mm lead followed by 1.5 mm aluminium walls. As described by ASTM Standards [4] these filter boxes eliminate dose enhancement effects caused by low energy photons. The facilities at LANL and UCSC allowed biasing and active monitoring of device performance during irradiations.

3. DETECTOR COMPONENT TESTS

3a. Detectors

We review [5] and report on new results from our systematic study of photon, neutron and proton radiation effects on single-sided AC-coupled silicon strip detectors. Our detectors were fabricated at SI (Oslo, Norway) on high resistivity n-type silicon wafers from Wacker Chemitronic (Burghausen, Germany). The wafer thickness was measured to be 290±10 μm [6]. The reverse bias voltage necessary for full depletion was determined from a measurement of the depletion layer capacitance to be 45 V, corresponding to a silicon bulk resistivity of 6 kΩcm. Each detector had 257 strips of 39 mm length with a pitch of 25 μm (Fig.1). All strips were covered with silicon dioxide and every second strip had an aluminium trace with bond pads for capacitively coupled readout. Each strip was terminated by a polysilicon resistor to a common bus line to provide the ground connection. A contact hole allowed access to the p-implant of each strip. There are three classes of strips: unmetallized, metallized without bonds, and metallized strips. (In bonded regions of the detector, only every second metallized strip was bonded out.) The active detector area of 2.55 cm^2 is defined by a surrounding guard diode.

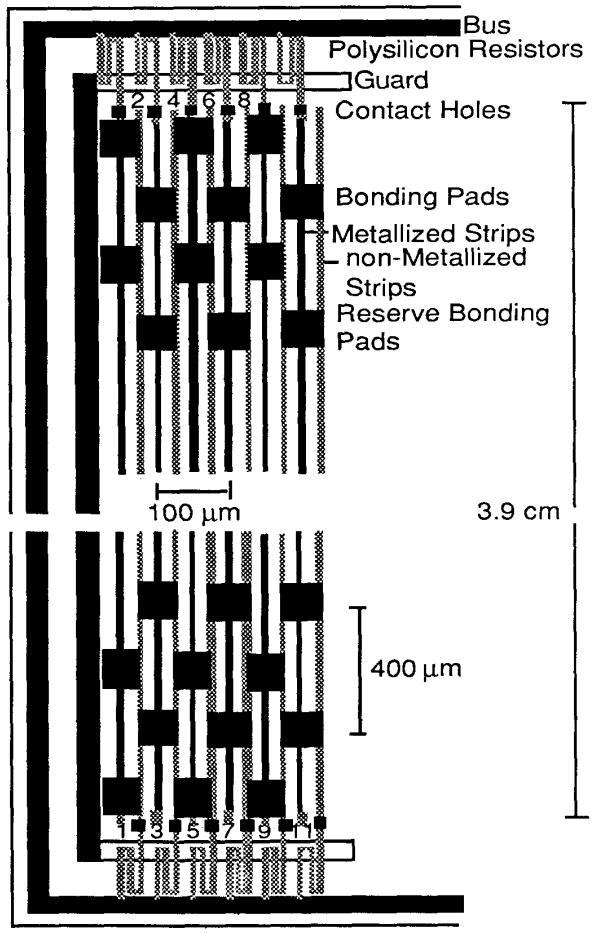

Fig. 1. Outline of the SI detector. Odd numbered strips are metallized

From the same wafers, test structures containing diodes, gated diodes, diffusion and polysilicon resistors, and MOS capacitors were fabricated. Additional tests of bulk damage in silicon were made using Hamamatsu 1723-06 PIN diodes. Nominally the devices are 1cm^2 in area, 200 μm thick, with a 170 μm thick depletion region, and are made of n-type high resistivity silicon (4 kΩcm). During the radiation exposures all detectors and test structure diodes were reverse biased at 40 V or 80 V. The photodiodes were either biased or had their leads shorted.

3b. Detector Currents

Initial leakage currents in excess of 0.2 nA per strip at 80 V bias voltage were found in only 4 out of 20 detectors. However, the current on the guard ring on 13 detectors was higher than 2 μA at 80 V bias. Detectors with guard currents of less than 0.1 μA were chosen for the radiation studies, but after gluing to printed circuit boards and bonding they showed guard currents of 50 to 100 μA. The guard current on one

detector was monitored during neutron irradiation and varied between 20 and 110 μA. Leakage currents of individual strips were measured on a probe station at a reverse bias voltage of 80 V. After neutron irradiation all three types of strips showed equal leakage currents (Fig. 2) as expected for bulk damage. After 3 weeks of annealing without bias at room temperature, those currents were reduced by only 9%.

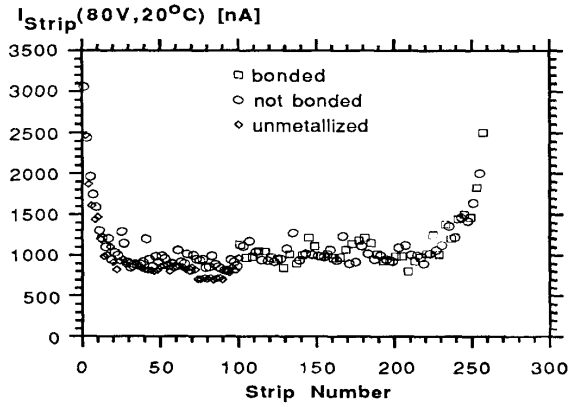

Fig. 2. Leakage current per strip after $9x10^{13}$ n/cm^2. Strips 101, 105,...,257 were bonded out.

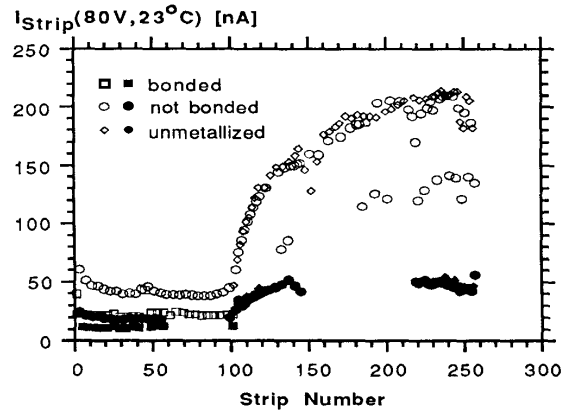

Fig. 3. Leakage current per strip immediately after 2.8Mrad ^{60}Co irradiation (open symbols) and after 6 days of annealing (filled symbols). Strips 1,5,9,...,99 were bonded out.

Figure 3 shows the leakage current per strip after a ^{60}Co dose of 2.8 Mrad. Photon-induced leakage currents are expected to be mainly due to surface effects. This agrees with the strong dependence of the observed leakage currents on the surface potential. The currents on neighboring bonded and floating metallized strips vary by a factor of 2. In the detector region without bonds, the currents on metallized and unmetallized strips are similar and a factor of 4 higher than in the bonded region. To study annealing the detector was kept biased at 40 V with the bonded strips grounded. After 6 days all strips showed the strong annealing typical of surface effects. The currents were reduced by a factor of 2 in the bonded region and by a factor of 4 in the floating region. At the SSC it is planned to bond all strips in order to minimize the leakage currents from surface effects. Our measurements indicate that the bulk generated leakage currents will dominate over surface and edge currents after one year of running at the design luminosity at the SSC.

3c. Polysilicon Resistors on Detectors

The polysilicon resistors on the detectors were about 500 nm thick, and boron doped to $2x10^{18}$/cm^3. In the present detector design, neighboring strips have their polysilicon resistors at opposite ends of the detector. Resistor values of 8.9 MΩ with less than 3% variation were measured at one end of the detector while values of 8.2 MΩ were measured at the other end, again uniform within 3% (Fig. 4). The length of the resistors at opposite ends are equal within two percent. The difference in resistor values must therefore be due to variations in polysilicon width or doping concentration. If those detectors developed leakage currents of 6 μA per strip the difference in resistor values would lead to a potential difference of 4.2 V between neighboring strips or the guard ring and could short them together by the punchthrough effect [7]. A lower value for the polysilicon resistors (*e.g.* 250 kΩ) should be used to avoid this problem. Under photon irradiation the resistor values increased by 15% and saturated after 0.2 Mrad (Fig. 5). The increase may be explained by the accumulation of fixed charges in the oxide underneath and on top of the resistors which leads to a partial depletion of the polysilicon [8]. The irradiation did not introduce any spread in resistor values on either end of the detector (Fig. 4). However, the difference in resistor values at opposite detector ends increased from 0.7 MΩ to 0.8 MΩ.

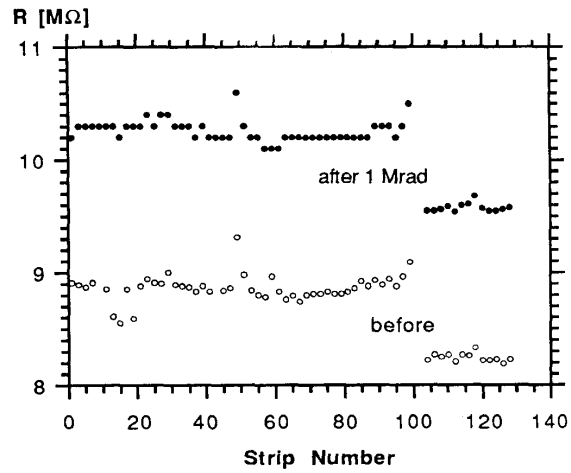

Fig. 4. Polysilicon resistor values before and after 1 Mrad of ^{60}Co irradiation. Strips above 100 (even numbered only) and below 100 (odd numbered only) have their resistors at opposite detector ends. (Note the zero suppression.)

3d. Test Structure Diffusion & Polysilicon Resistors

In addition to the polysilicon resistors on the detectors, we studied the polysilicon and diffusion resistors on the test structures. Their values were monitored during exposures to total fluences of $\approx 3\times10^{13}$n/cm^2 and $\approx 9\times10^{14}$p/cm^2 and are shown in Fig. 6, 7. Under the neutron irradiation, the polysilicon resistors remained unchanged. The diffusion resistors showed an initial increase of approximately 5%, followed by a much slower increase of $\approx 0.3\%/10^{13}$n/cm^2. Under the proton irradiation just the opposite behavior was seen. The polysilicon resistors show a sharp initial increase in resistance of approximately 7.5% indicative of surface damage. That was followed by a much slower and linear increase with total dose of $\approx 0.2\%/10^{14}$p/cm^2. The diffusion resistors show a similar small long term increase in resistance but show no initial jump. All the observed changes are negligible from the viewpoint of detector operation.

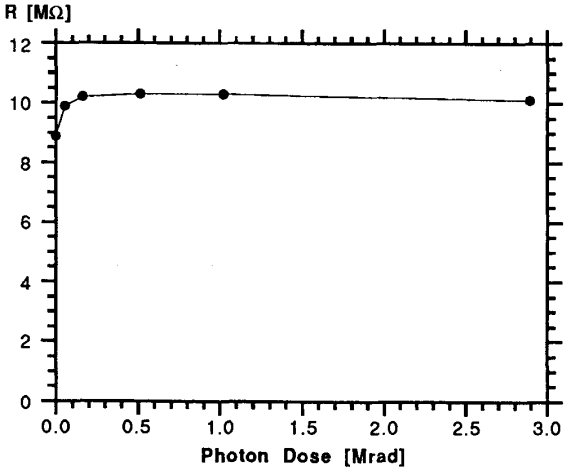

Fig. 5. Polysilicon resistor values under ^{60}Co irradiation.

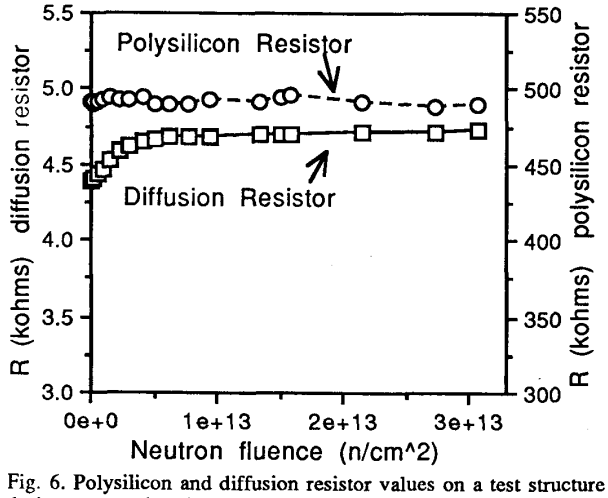

Fig. 6. Polysilicon and diffusion resistor values on a test structure during neutron irradiation. (Note the zero suppression.)

3e. Coupling Capacitors

The coupling capacitors are formed by a layer of silicon dioxide and an aluminum trace covering the full length and width of each strip. An oxide thickness of 250 nm was calculated from a capacitance of 44.5 pF. The coupling capacitors on each strip were uniform to better than 1% (Fig.8). After 2.8 Mrad of photon irradiation the coupling capacitors did not change within the measuring accuracy of 0.2 pF (Fig.8). Neither did they change after neutron irradiation (Fig. 9). No significant change in leakage current or breakdown voltage was seen after exposure to $\approx 9\times10^{14}$p/cm^2.

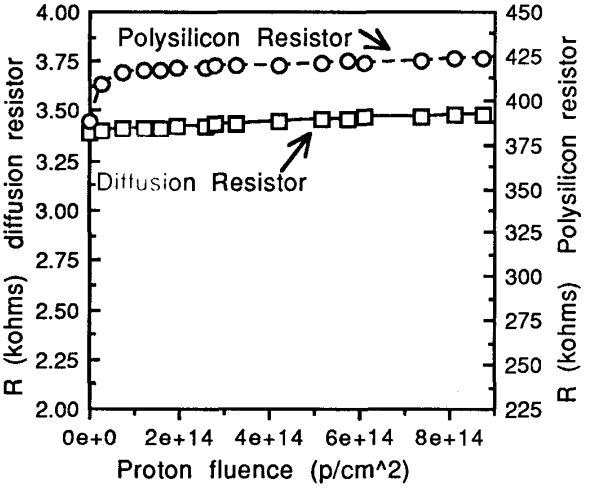

Fig. 7. Polysilicon and diffusion resistor values on a test structure during proton irradiation. (Note the zero suppression.)

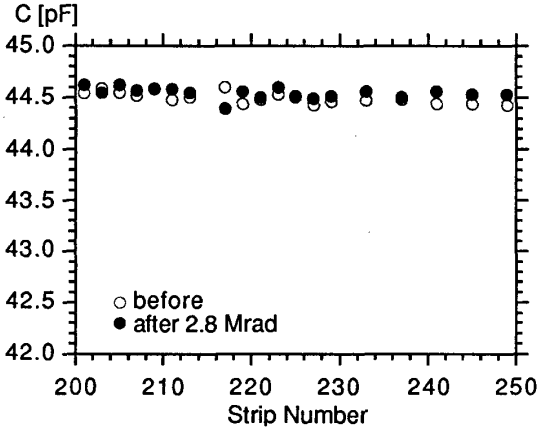

Fig. 8. Coupling capacitors before and after 2.8 Mrad ^{60}Co irradiation, measured with 0.2 pF resolution.

3f. Oxide Charges

The test structures contained a MOS capacitor with an area of A=20 mm^2 and an oxide thickness of 500 nm, calculated from the measured oxide capacitance C_{ox}. Both capacitor

contacts were grounded during irradiation. Comparing C-V curves measured before and after photon irradiation (Fig. 10) we observe a "shift" due to fixed oxide charges and some "stretching" due to interface charges. To separate those contributions, the midgap-capacitance was calculated to be 230 pF [9] and the shift in midgap voltage ΔV_{mg} was determined from the C-V curves. The oxide charge density Q_{ox} is given by

$$Q_{ox} = eN_{ox} = C_{ox}\Delta V_{mg} / A. \quad (3)$$

The oxide charge density reached the well known saturation value of $2.5 \times 10^{12}/cm^2$ after a few hundred krad [10,11] (Fig. 11). After three days of annealing at room temperature and with zero bias voltage the oxide charge density was reduced by a factor of two.

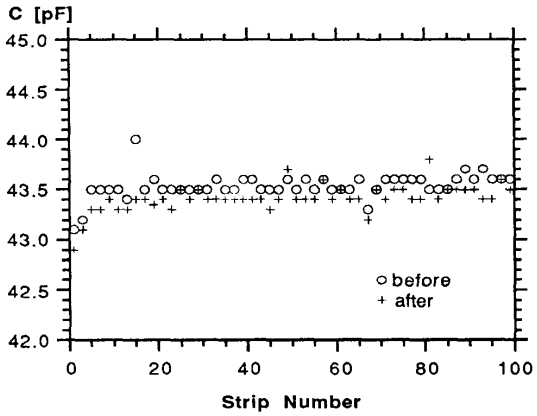

Fig. 9. Coupling capacitors before and after 9×10^{13} n/cm^2.

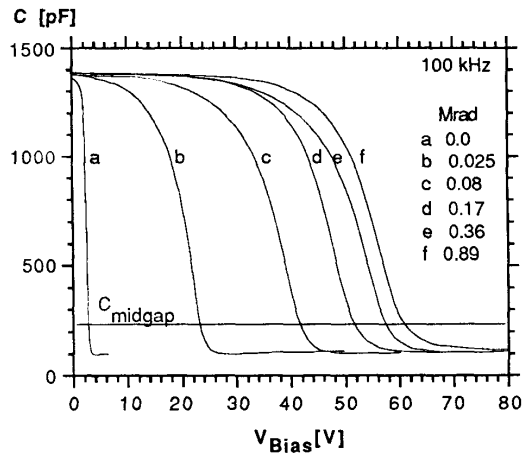

Fig. 10. C-V curves at 100kHz for an MOS capacitor under ^{60}Co irradiation with zero bias voltage. The calculated midgap capacitance is indicated.

4. BULK DETECTOR EFFECTS

4a. Acceptor site creation

Displacement damage appears to lead to the creation of positively charged acceptor sites throughout the bulk of a silicon detector. That process changes the effective dopant levels in the silicon. For the radiation doses expected at the SSC, the effect only impacts the lightly doped ($\sim 10^{12}/cm^3$) bulk depletion region which comprises the sensitive volume of the detector. The heavily doped ($\sim 10^{18}/cm^3$) contact regions are essentially unaffected by the acceptor creation. The lightly doped n-type material of which most detectors are made, is slowly turned into fully compensated material, as the newly created acceptor sites effectively neutralize the donor sites in the original n-type material. As yet more acceptor type states are created the material becomes p-type (undergoes inversion). As the number of acceptor states continues to increase, the material becomes more heavily doped p-type of ever decreasing resistivity. The decrease in resistivity translates directly into an increase in the voltage needed to deplete the detector. That eventually leads to depletion voltages which create local electric field strengths greater than can be maintained in silicon, resulting in breakdown of the detector, or its forced operation in a mode where it is not fully depleted.

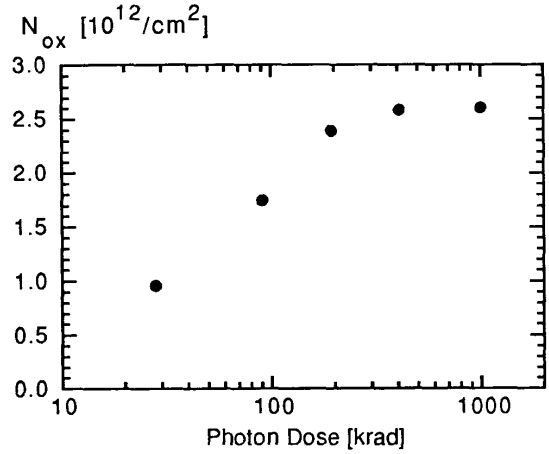

Fig. 11. Oxide charge density in SiO_2 under ^{60}Co irradiation.

Using the symbol definitions given below, the depletion depth of a silicon detector (d) is given in equation (4).

N_o = the donor concentration in the original n-type material,
Φ = fluence in particles/cm^2,
ß = damage constant (acceptor states/cm/incident particle),
ε = dielectric constant for silicon = 1.054 pF/cm,
V_d = bias voltage for depletion, and
q = lelectron chargel.

$$d = (2\varepsilon V_d/qN)^{1/2} \quad (4)$$

The number of acceptor states (holes) created is assumed to be linearly proportional to the fluence and is thus

$$N = |N_o - \Phi\beta| \quad (5)$$

Combining equations (4) and (5) and solving for V_d one finally has

$$V_d \approx qd^2|N_o - \Phi\beta|/2\varepsilon \quad (6)$$

4b. Determination of ß:

The depletion voltage of a silicon detector can be determined from a measurement of the depletion layer capacitance as a function of the reverse bias voltage (see Fig. 12). That was done for the Hamamatsu photodiodes at several different times during the proton irradiation. In Fig. 13 we show the data and the expected V_d dependence on Φ for several values of β. We note that a value of β_p = (0.05±0.01)/cm gives a good fit to the data. We remeasured the full depletion voltage of the diodes 20 days after their removal from the beam and found that the depletion voltage decreased by approximately a factor of two. At later times, no additional annealing was observed.

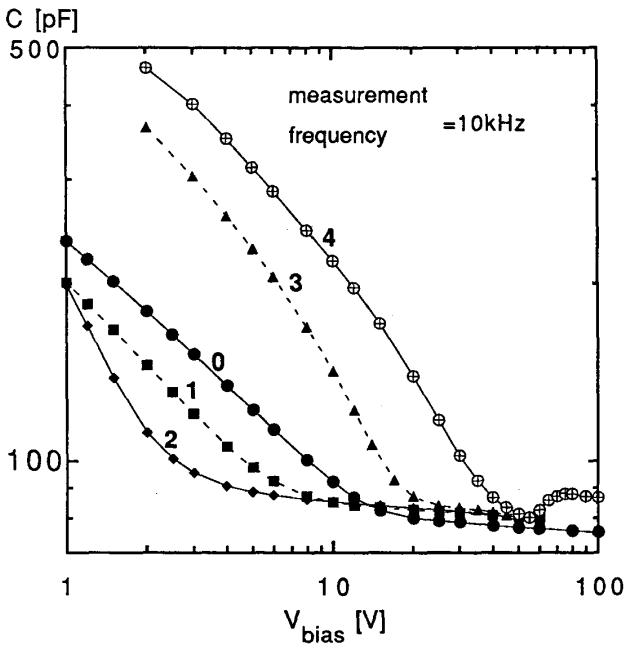

Fig. 12. Capacitance as a function of bias voltage for Hamamatsu photodiodes for different proton fluences. {0=initial, 1→4 are for different (increasing) proton fluences.}

4c. Leakage Current Damage Constant

We have determined the leakage current damage constant α, which relates the leakage current density J to the fluence Φ,

$$J = \alpha\Phi + J_o \quad (7)$$

for 800 MeV protons using the Hamamatsu photodiodes. Fig. 14 shows the relation between leakage current and fluence. We determine $\alpha = (4.8\pm0.5)\times10^{-17}$ A/cm. {Our previous result [12] of $\alpha = 4.0\times10^{-17}$ A/cm scales to 4.4×10^{17} A/cm when one uses the newer value [13] for the 800 MeV production cross section $^{27}Al + p \rightarrow {}^{22}Na + X$, which we use in the present paper.}

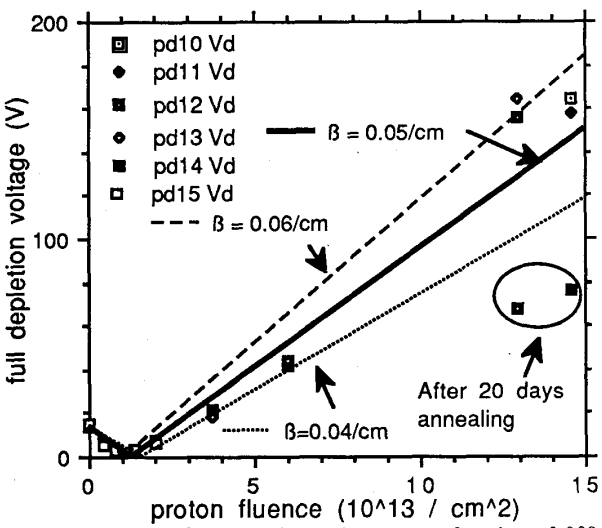

Fig. 13. Measured full depletion voltages as a function of 800 MeV proton fluence. The lines are the results of calculations using equation (6) for different values of β. An initial donor concentration of $6.4\times10^{11}/cm^3$ and a full depletion depth of 170 µm were assumed.

4

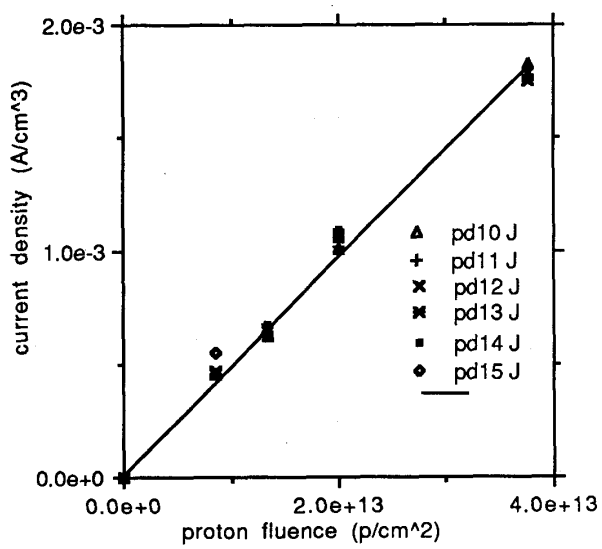

Fig. 14. Leakage current density in Hamamatsu photodiodes as a function of 800 MeV proton fluence. The line is a plot of equation (7) for $\alpha = 4.8\times10^{-17}$ A/cm.

4d. Detector Survival:

Applying the value of $\beta_p = 0.05/cm$ determined above, we observe the following: for a 300 μm thick silicon detector, with initial n-type doping of $2.5 \times 10^{12}/cm^3$ the full depletion voltage is 170 V. This detector inverts to p-type after a charged particle fluence of $5.0 \times 10^{13}/cm^2$ and after $1.0 \times 10^{14}/cm^2$ the full depletion voltage is again 170 V. The observed annealing would roughly double the fluence (and hence time) required to cause that change. The leakage current for a 50 μm by 6 cm long strip at that dose is about 3.6 μA (20°C). (If the detector was operated at 0°C the leakage current would be reduced to 0.55 μA.) The fluence of $1.0 \times 10^{14}/cm^2$ corresponds to the maximum dose expected for a silicon microstrip detector at the SSC in one decade of operation at the design luminosity.

5. RADIATION TESTS OF FRONT-END ELECTRONICS

We have previously reported on our progress in identifying radiation hard technologies [12,14,15], and we will give here only an update. Because of the high collision frequency at the SSC and the very large channel count, we are considering a "digital" read-out system that records for every beam crossing only the addresses of the strips with pulse height above a certain threshold. Considerations of signal-to-noise and power consumption will possibly lead to a system with mixed technologies: bipolar for the analog amplifier/comparator chip (AACC), and CMOS for the digital buffer chip (DTSC).

The design of an AACC is described in Ref. [16]. The chip has been designed out for 64 channels at 85 μm pitch in dielectric isolation (D.I.) bipolar technology in a full custom process developed by Silicon Dynamics, Inc.[17], and initial fabrication has just been completed. In order to examine the radiation hardness of devices produced using the D.I. technique we have tested such transistors (made on the backside of wafers produced by AT&T) under neutron exposure at LASREF. We were concerned about in a possible degradation of the current gain β with large neutron fluences. Fig. 15 shows the result of the test: After fluences of 9×10^{13} n/cm^2, β had changed by only approximately 10%, even for very small current densities. That indicates the bipolar D.I. transistors exhibit sufficient radiation hardness for experimentation at the SSC.

The design of a DTSC is described in Ref. [18]. For low power consumption, the DTSC is designed using SRAM's and is implemented in CMOS. A test version has been manufactured in radiation-hard 1.2 μm CMOS by UTMC [19]. Test structures on the chip have been irradiated to test the radiation hardness of the design. Fig. 16 shows the threshold shift ΔV_{th} of p and n transistors, and Fig. 17 the change in the transition voltage ΔV_G of a NAND gate and INVERTER after doses of up to 3.2Mrad of ^{60}Co exposures. The transistors show the expected small shifts in V_{th} [12], while the logic gates exhibit a much smaller change, because the effects on the n and p transistors compensate each other. As observed before [12], the damage saturates at large doses. Another device tested for radiation damage was a ring oscillator. We measured the oscillation frequency of a 51 stage ring oscillator and found a frequency of 34.0 MHz before, and 32.6 MHz after irradiation with 3.2 Mrad ^{60}Co. Radiation tests of the DTSC itself are just beginning.

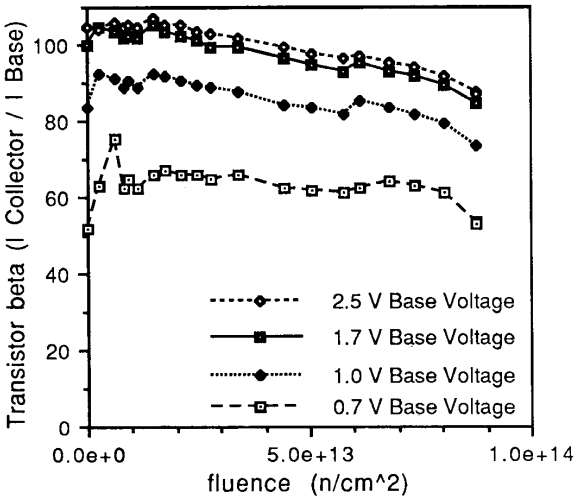

Fig. 15. Variation of the current gain β of dielectric isolation bipolar transistors as a function of the neutron fluence.

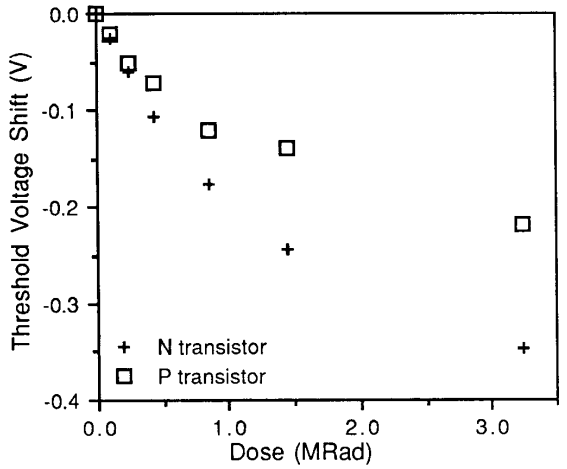

Fig. 16. Shift of the threshold voltage as a function of ^{60}Co dose for representative n and p transistors in the DTSC chip.

6. CONCLUSIONS

The individual components of AC-coupled silicon strip detectors, as well as the components of both CMOS and bipolar front-end electronics show sufficient radiation tolerance for operation for periods in excess of one decade as parts of a silicon microstrip detector system at the SSC. Bulk damage to the silicon itself is seen as the limiting factor in the lifetime

of a detector system. In particular, it is the acceptor site creation in the active volume of the silicon detector that will limit the lifetime to approximately 10 years for the inner most detectors. That effect will need further investigation.

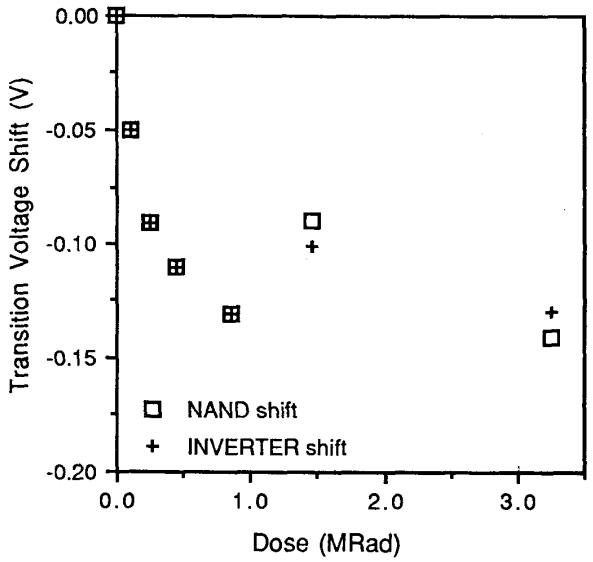

Fig. 17. Shift of the transition voltage of the NAND gate and the INVERTER built with the transistors of Fig. 16.

7. REFERENCES

[1] D.R. Davidson *et al.*, J. Nucl. Matl. **122&123**, 989, (1984), M.S. Wechsler et al. , J. Nucl. Matl. **122&123**, 1078, (1984).

[2] M. Hasegawa *et al.*, Nucl. Instr. and Meth. **A277** 395 (1989).

[3] T. Ohsugi *et al.*, Nucl. Instr. and Meth. **A265** 105 (1988).

[4] 1990 Annual Book of ASTM Standards, Vol 12.02 (Nuclear(II), Solar and Geothermal Energy), Standard E 1249. American Society for Testing and Materials, Philadelphia (1990).

[5] D. Pitzl *et al.*, 2nd Conference on Advanced Technology and Particle Physics, Como, Italy, June 1990.

[6] G. Hall, Imperial College, private communication and L. Evensen, SI, private communication.

[7] J. Ellison *et al.*, IEEE Trans. Nucl. Sci. **NS-36** 267 (1989).

[8] L. Bosisio, Pisa, private communication.

[9] S. M. Sze, Physics of Semiconductor Devices, 2nd Ed., Wiley 369 (1981).

[10] E. H. Snow *et al.*, IEEE Proc. **55** 1168 (1967).

[11] T. P. Ma, P. V. Dressendorfer (Eds.), Ionizing Radiation Effects in MOS Devices and Circuits, Wiley 1989.

[12] H. Ziock *et al.*, IEEE Trans. Nucl. Sci. **NS-37**, 1238 (1990).

[13] H.R. Heydegger *et al.*, Phys. Rev. **C14** 1506 (1976).

[14] H.F.-W. Sadrozinski, SCIPP 90/02; G. Hall, Imperial College Note IC/HEP/90/1.

[15] H.F.-W. Sadrozinski, *et al.*, 2nd London Conference on Position Sensitive Devices, London, U.K., September 1990.

[16] D.E. Dorfan, Nucl. Instr. and Meth. **A279** 186 (1989).

[17] Silicon Dynamics Inc., Ames, IA, 50010 USA.

[18] J. DeWitt, Nucl. Instr. and Meth. **A288** 209 (1990).

[19] United Technologies Microelectronic Center (UTMC), Colorado Springs, CO, USA.